HYDROLOGICAL PROCESSES
Hydrol. Process. **18**, 2851–2875 (2004)
Published online 30 June 2004 in Wiley InterScience (www.interscience.wiley.com). DOI: 10.1002/hyp.1498

Identifying Storm Flow Pathways In A Rainforest Catchment Using Hydrological and Geochemical Modelling

David A. Kinner[1,2]* and Robert F. Stallard[1]

[1] *U.S. Geological Survey-WRD, 3215 Marine Street, Boulder, CO 80303,*
[2] *Institute of Arctic and Alpine Research, Boulder, CO 80302-0450, USA*

Abstract:

The hydrological model TOPMODEL is used to assess the water balance and describe flow paths for the 9·73 ha Lutz Creek Catchment in Central Panama. Monte Carlo results are evaluated based on their fit to the observed hydrograph, catchment-averaged soil moisture and stream chemistry. TOPMODEL, with a direct-flow mechanism that is intended to route water through rapid shallow-soil flow, matched observed chemistry and discharge better than the basic version of TOPMODEL and provided a reasonable fit to observed soil moisture and wet-season discharge at both 15-min and daily time-steps. The improvement of simulations with the implementation of a direct-flow component indicates that a storm flow path not represented in the original version of TOPMODEL plays a primary role in the response of Lutz Creek Catchment. This flow path may be consistent with the active and abundant pipeflow that is observed or delayed saturation overland flow. The 'best-accepted' simulations from 1991 to 1997 indicate that around 41% of precipitation becomes direct flow and around 10% is saturation overland flow. Other field observations are needed to constrain evaporative and groundwater losses in the model and to characterize chemical end-members posited in this paper. Published in 2004 by John Wiley & Sons, Ltd.

KEY WORDS tropics; hydrology; flowpaths; TOPMODEL; end-member chemical mixing

INTRODUCTION

Water from rainfall is delivered to streams through a variety of flow paths, each affecting runoff style, soil erosion and nutrient cycling. The importance of a particular flow path depends on the soils, topography and climate of a catchment. Fast flow paths such as soil pipes and saturation overland flow deliver peak flows to the channel on time scales of minutes to hours for catchments with areas of about 10 ha (Jones, 1997; Elsenbeer and Vertessey, 2000). Slow flow-paths in the soil matrix deliver water (throughflow) to the channel at time-scales of hours to days (Jones, 1997). During a rainstorm, the different pathways interact such that distinctions among individual flow paths are gradational (Elsenbeer *et al*., 1995; Elsenbeer and Vertessey, 2000).

Fast and slow flow-paths in tropical catchments can be differentiated on the basis of water chemistry. At La Cuenca in Peru (Elsenbeer *et al*., 1995) and in South Creek, Queensland (Elsenbeer *et al*., 1994) water emerging from fast flow-paths had a high potassium (K^+) concentration relative to slow flow-paths. By tracking the chemical composition of water as it moved through the soil, they concluded that the high K^+ concentration was generated by contact with canopy and litter biomass. Concomitantly, Elsenbeer *et al*. (1995) measured the highest concentrations of calcium (Ca^{2+}), magnesium (Mg^{2+}) and silica ($Si(OH)_4$) in valley groundwater and seeps.

Elsenbeer (2001) suggested that the hydrological response of tropical catchments lies on a continuum based on the vertical permeability profile of the catchment's soils. One end-member of the continuum includes

* Correspondence to: David A. Kinner, Institute of Arctic and Alpine Research, Boulder, CO 80302-0450, USA.
E-mail: dakinner@usgs.gov

Received 28 April 2003
Accepted 19 September 2003

catchments with Acrisol soils. Acrisols in the tropics have up to a two to three order of magnitude reduction in permeability within the first meter of depth. In tropical settings, this zone of high permeability is the result of both pedological processes (i.e. soil fauna, clay illuviation) and the high density of roots at the soil surface (Dietrich *et al*., 1982; Larsen and Torres-Sanchez, 1990). The other end-member is a Ferralsol soil catchment that has a modest (one order of magnitude or less) decrease in permeability within the first metre of depth (e.g. Elsenbeer and Lack, 1996, figure 43.2).

The pronounced reduction in permeability with depth in tropical Acrisol soils leads to a characteristic suite of hydrological processes and the dominance of fast flow-paths during storms. Infiltrating water ponds at the base of the root zone, forming a perched water table (Bonell and Gilmour, 1978; Elsenbeer, 2001). Molicova *et al*. (1997, figures 6 and 7) measured a shallow, perched water table in French Guiana using tensiometers. Elsewhere (e.g. La Cuenca in Peru), perched water is inferred by the response times of soil-pipe networks (Elsenbeer and Lack, 1996, figure 43.10). These shallow water tables can extend to the surface providing saturation-excess and return components of saturation overland flow. They may also drain through soil pipes that may in turn have overland flow at their outlets. Ferrasol landscapes often have pipe networks, but there is less pipeflow than in Acrisol landscapes because there is no ponding to force water into the pipes (Elsenbeer and Lack, 1996).

In the present study, flow paths are examined for a catchment in a Panamanian tropical forest catchment, Lutz Creek Catchment (Figures 1 and 2) located on Barro Colorado Island (BCI) in Panama. The research hypothesis for the paper is that, because Lutz is an Acrisol soil catchment, then pipeflow and saturation overland flow are the main runoff processes generating the stormflow response to rainfalls. Previous pedologic and hydrometric evidence supports this assertion (Dietrich *et al*., 1982; Keller, unpublished manuscript, 1985). Through field mapping, Keller (unpublished manuscript, 1985) indicated that soils in Lutz Creek Catchment were Cambisols, making them similar to the Acrisol end-member. Additionally, he measured a difference in bulk density from 0·7 g/cm^3 at the surface to 1·1 g/cm^3 at a depth of 1·25 m. Dietrich *et al*. (1982) utilized soil moisture records to conclude that the surface soil was near saturation for over half the year. Kursar *et al*. (1995) supported this assertion by measuring soil-water potentials of 0 MPa for much of the wet season in similar soils elsewhere on BCI. Dietrich *et al*. (1982) suggested that this near-surface saturation provided source areas for saturation overland flow. Dietrich *et al*. (1982) also estimated that 20% of the annual hydrograph was overland flow; they did not consider the potential importance of pipeflow in hydrological response, as its significance in many hydrological settings had not yet been fully established in 1982.

Recent video footage from Lutz Creek Catchment taken 11 January 2002 (S. Paton, personal communication) provided qualitative evidence for similarity between Elsenbeer's (2001) Acrisol end-members and Lutz Creek Catchment. A large storm on 17–18 November 2001 caused channel bank failures throughout the catchment and exposed a large network of soil pipes, some almost 0·1 m in diameter. The video showed substantial pipeflow in the catchment even though it had been several days since the prior rain. The estimated density of soil pipes per exposed bank area was of the order of one substantial pipe per square metre.

The present paper seeks to model the hydrology of Lutz Creek. Hydrological models of catchments provide a powerful bridge between hydrology and other scientific disciplines that may be asking water-related questions in the same catchments. For Lutz Creek, many of these questions are also being asked by biologists, including ecologists, plant physiologists and soil biologists. Soil moisture status and the aqueous transport of plant nutrients (nitrate, ammonia, phosphates, and potassium) are common concerns.

Gridded hydrological models permit reconstruction of soil moisture status over an entire catchment and surrounding areas. TOPMODEL (Beven and Kirkby, 1979) is used in this paper, but it is acknowledged that other models may be similarly suited. The Lutz Catchment hydrology is modelled using two time-steps. The short time-step (15 min) is used to help determine the processes that dominate storm runoff. A second daily time-step is used in an attempt to verify whether results from the short time-step are reasonably like those derived from the longer time-step. The daily interval is typical of the large, long-term precipitation data sets used by researchers in most tropical regions. For example, the daily precipitation data for Lutz Catchment goes back to 1925 (Windsor, 1990).

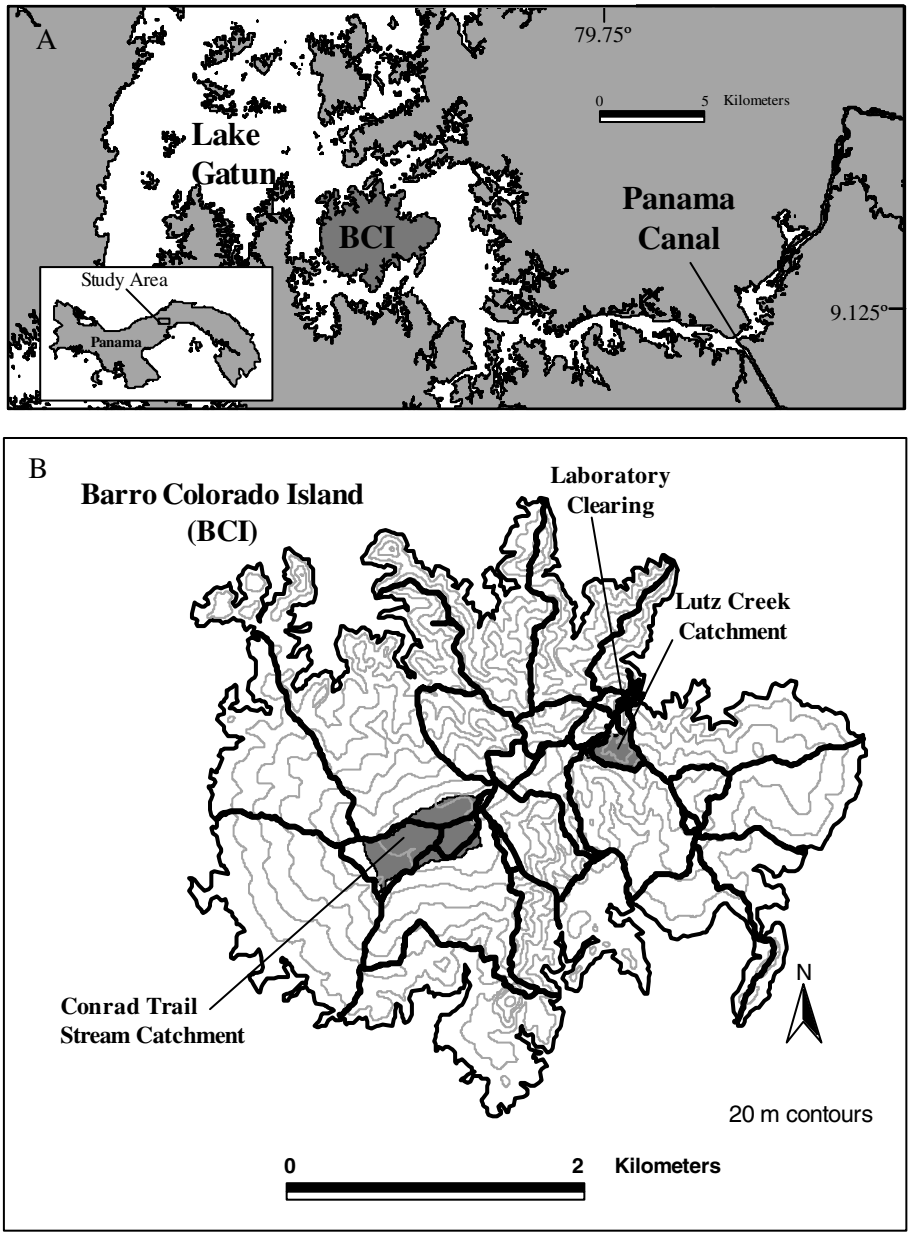

Figure 1. (A) Map of the central Panama Canal region indicating the location of Barro Colorado Island (BCI) relative to the Panama Canal and Lake Gatun. (B) Contour map of BCI showing 20-m contours (grey lines), the island walking trail network (thick black lines), the locations of two hydrological research catchments (Lutz Creek and Conrad Trail Stream), and the location of the island laboratory clearing

Setting

Barro Colorado Island (Figure 1) is covered by a tropical, semi-deciduous moist forest in several successional stages (Foster and Brokaw, 1982). The island was formed in 1914 with the creation of Lake Gatún as part of the Panama Canal. It is 1500 ha, with a summit plateau at 164 m elevation (137 m above lake level). Island climate consists of distinct wet and dry seasons and a total rainfall averaging 2600 mm/year (1925

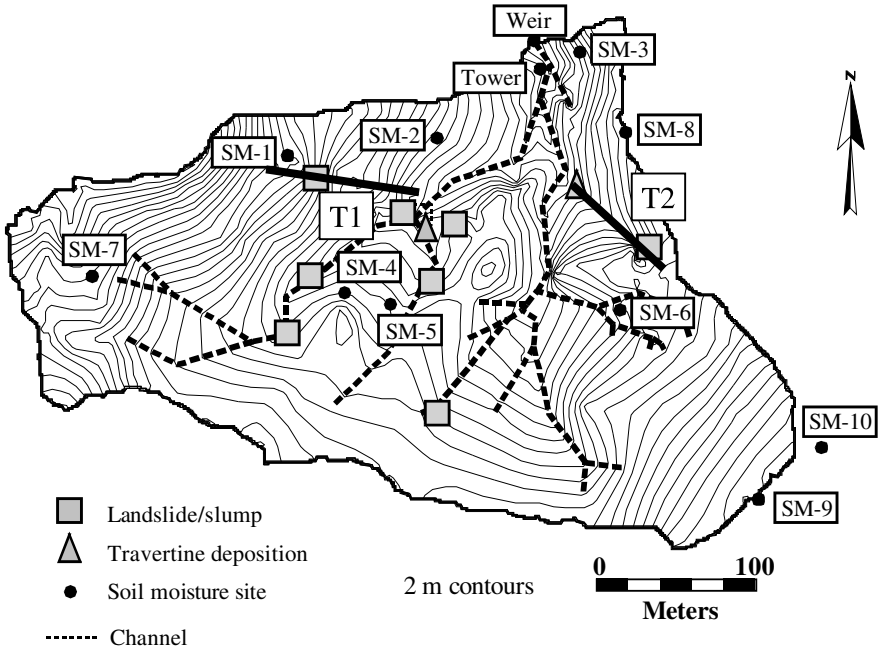

Figure 2. Contour map of Lutz Creek catchment based on field surveys. The map includes the location of channels, landslides/slumps, travertine, transects ([T1], [T2]) and the 10 biweekly soil moisture measurement locations

to 1998) (Windsor, 1990; S. Paton, unpublished data, 1998). The pronounced dry season is approximately mid-December to the end of April and the wet season is approximately May to mid-December. On average, only 285 mm of rain falls in the dry season. Most meteorological variables exhibit marked wet/dry season differences; however, mean daily temperature varies little throughout the year (Windsor, 1990).

The 9·73 ha Lutz Creek Catchment is located near the island laboratory (9°10'N, 79°51'W). Monitoring of catchment hydrology began in the early 1970s and consists of discharge measurements taken at 5-min intervals (Windsor, 1990). Precipitation is measured using a tipping bucket rain gauge on the 40-m canopy tower within the catchment and in a calibrated NOAA-type gauge in the 'laboratory clearing' adjacent to the catchment (Figures 2 and 1, respectively). Because the latter gauge registered consistently higher rainfall than the tipping bucket, tipping bucket data were scaled to equal the daily totals from the NOAA gauge. Soil moisture is also collected biweekly on a 10-site circuit (Windsor, 1990). Grab samples and event samples collected by an ISCO (the use of trade, product or firm names in this paper is for descriptive purposes and does not imply endorsement by the U.S. Government) sampler were analysed for major constituents (Na^+, K^+, Ca^{2+}, Mg^{2+}, $Si(OH)_4$, Cl^-, $SO_4{}^{2-}$, alkalinity), nutrients (NO_{2^-}, NO_{3^-}, $NH_4{}^+$, $PO_4{}^{3-}$), and dissolved organic carbon (DOC).

Three lithological units underlie Lutz Creek Catchment: the Bohio Formation and the Marine and Volcanic Facies of the Caimito Formation. The older Bohio is a volcaniclastic matrix-dominated conglomerate and the Caimito Marine Facies is a sandstone with calcic cement and, locally, pieces of pelecypodal limestone (Woodring, 1958). The Caimito Volcanic Facies is a fine-grained volcaniclastic sandstone that constitutes 5% of the study area. Island geology is described extensively in Woodring (1958) and Johnsson and Stallard (1989).

Dietrich *et al*. (1982) suggested that the erosion rate in Lutz Creek Catchment is about 0·75 mm/year. The numerous landslide scars, smaller channel-side slumps and bank failures (Figure 2) provide material for denudation. The mass wasting is sustained by chemical weathering dominated by dissolution of carbonate cements. The Mg-rich groundwater fosters the formation of montmorillonite and associated expansive soils

(Johnsson and Stallard, 1989). Travertine terraces, mapped in Figure 2 and 10-m downstream from the weir, are actively forming.

METHODS

The work in this paper consists of a number of interrelated activities including assembling the available hydrological, geochemical and meterological data for the catchment, field mapping and calculation of field soil hydraulic conductivity using Guelph permeametry, and TOPMODEL modelling. The concept is to integrate as many sources of data as possible to examine flow-path and daily water-balance issues. Field activities, model input data and the modelling approach are described in this section.

Field mapping and Guelph permeability tests

Field mapping included a survey of approximately 1000 spot elevations that were used to generate the topographic map in Figure 2. Included in these elevation points were surveys along channels to allow for accurate calculations of stream hydraulic gradients. The information was gridded at a 5-m resolution using the TOPOGRID algorithm in Arc-Info™ to create a digital elevation model (DEM).

Two representative topographic transects were examined in detail (Figures 2 and 3). The western transect is a Bohio Formation slope sequence (T1), and the eastern transect is a Caimito Formation slope sequence (T2). At five points along each transect, the saturated hydraulic conductivity (K_{sat}) of the soil was measured using a Guelph Permeameter (Soil Moisture Equipment Corp, 1986) for shallow (5–15 cm) and deeper soil horizons (20–30 cm). At each location we measured radial flow from a borehole at multiple heads. The analytical solution provided with the Guelph Permeameter and derived by Reynolds *et al*. (1983) yielded negative values of hydraulic conductivity. This probably is the result of vertical heterogeneity in the soil profile (Reynolds and Elrick, 1985). Accordingly, we used the one-head Laplacian equation of Reynolds and Elrick (1985) to convert flux measurements to hydraulic conductivity estimates. Soil descriptions and derived values of hydraulic conductivity are listed in Table I.

The soils of the two transects matched the structure of the parent material. The Caimito Formation soils, derived from a sandy calcic matrix, formed a thick clay above a sandy saprolite. The Bohio Formation soils, derived from a conglomerate, locally had the original clasts of the conglomerate that weathered to a sand surrounded by a thick clay matrix.

There were considerable, non-systematic variations in hydraulic conductivity ($n = 18$). Values for K_{sat} ranged from 13 mm/h at Camito Site 4 to 0·008 mm/h at Bohio Site 4 (Table I). With such a small suite of measurements, we were unable to resolve the spatial or vertical pattern of hydraulic conductivity. Additionally, the technique prohibited us from measuring the permeability of the surface soil. Some sites had greater values of K_{sat} at depth whereas others have higher values of K_{sat} at the surface. In Bohio Formation soils, particularly at site 1B, a gravel layer controlled the permeability of the lower measurement (0·55 m). This suggests that, in addition to macropores, the heterogeneity in the conglomerate parent-material and differential weathering may generate preferential flow paths. A larger, more systematic suite of measurements is needed to understand the patterns of hydraulic conductivity in Lutz Catchment soils. Further, the use of other types of infiltration tests may be necessary to simulate the effects of rainsplash on infiltration in Lutz Creek Catchment.

Organisms and seasonal moisture variations affect soil structure and properties. In soils located on a southern peninsula of BCI that are physically and chemically similar to those in Lutz Creek Catchment, mean infiltration rates measured by a double-ring infiltrometer ranged from 1800 mm/h in the dry season to 200 mm/h in the wet season (Kursar *et al*., 1995). This seasonal contrast is the result of dry-season soil cracking and bioturbation, which open additional pathways for infiltrating moisture, followed by wet-season collapse (Smela, 1987; Kursar *et al*., 1995). The minimum volume percentage moisture of these soils is 19%, and the field capacity is 30% (Kursar *et al*., 1995).

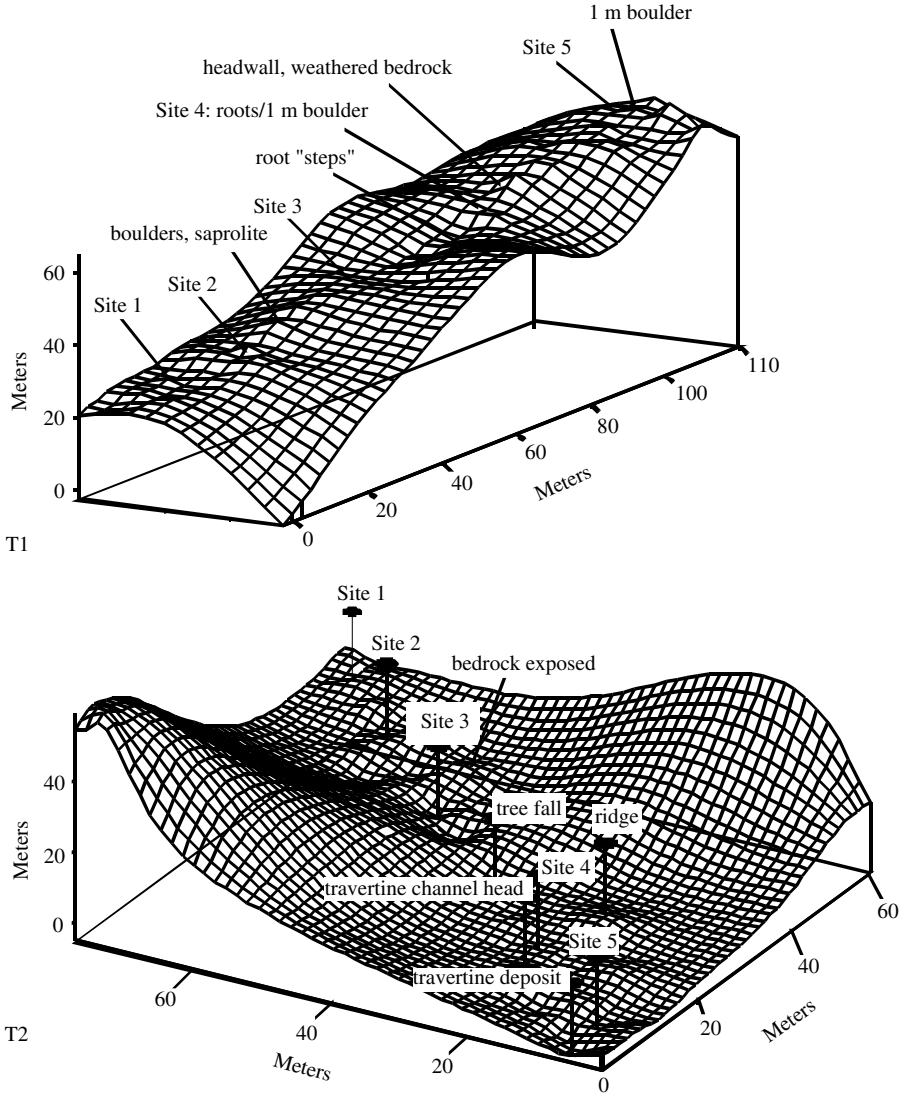

Figure 3. Three-dimensional representations of Bohio Formation (T1) and Caimito Formation (T2) transects. Locations of hydraulic conductivity boreholes and other observed features are shown. Axis location is relative to a local arbitrary datum

Calculating potential evapotranspiration

All of the meteorological data necessary to calculate potential evapotranspiration (PE) using the Penman–Monteith formula are collected in the canopy tower and the laboratory clearing. Potential evaporation also has been measured directly since 1994 using both an evaporation pan in the clearing and an atmometer positioned on top of the 40-m canopy tower (S. Paton, unpublished data, 1998). Estimates from the canopy tower atmometer during 1994–1997 place the mean yearly potential evapotranspiration at 1341 mm.

We used the same version of the Penman–Monteith formula as was applied by Dietrich *et al*. (1982) to estimate PE during years for which no atmometer measurements are available (1991–1993). To determine whether our usage of the Penman–Monteith formula is appropriate, daily PE measured with an atmometer from the years 1994–1997 were compared with the Penman–Monteith predictions (Table II). The cumulative

Table I. Field measurements of hydraulic conductivity and description of soil field properties at 10 transect points in Lutz Creek Catchment

Location	Depth (cm)	K_{sat} (mm/h)[a]	Texture[b]	Munsell colour	Percentage moisture by mass[c]
Bohio-1	17	$6{\cdot}60 \times 10^{-2}$	Sandy loam	10 YR 3/2	35·7
	55	$4{\cdot}27 \times 10^{0}$			
Bohio-2	17	$0{\cdot}85 \times 10^{-1}$	Sandy clay loam	10 YR 3/2	33·3
	30	$3{\cdot}25 \times 10^{0}$			
Bohio-3	17	$3{\cdot}79 \times 10^{-1}$	Sandy loam	5 YR 4/2	35·5
Bohio-4	10	$8{\cdot}64 \times 10^{-3}$	Sandy clay loam	5 YR 4/3	37·8
	30	$7{\cdot}32 \times 10^{-2}$			
Bohio-5	9	$1{\cdot}26 \times 10^{-1}$	Sandy loam	10 YR 3/2	32·5
	25	$5{\cdot}28 \times 10^{-1}$			
Caimito-1	9	$1{\cdot}08 \times 10^{-1}$	Clay loam	7·5 YR 3/2	41·1
Caimito-2	13	$3{\cdot}96 \times 10^{-2}$	Clay loam	10 YR 3/2	45·4
	30	$1{\cdot}08 \times 10^{-1}$			
Caimito-3	30	$1{\cdot}6 \times 10^{-2}$	Sandy clay loam	10 YR 3/1	44·7
Caimito-4	28	$1{\cdot}32 \times 10^{1}$	Clay loam	10 YR 3/1	46·9
Caimito-5	24	$6{\cdot}06 \times 10^{-1}$	Clay loam	10 YR 3/3	41·0

[a] Measured with Guelph Permeameter and estimated using Laplace formula of Reynolds and Elrick (1985).
[b] Based on field criteria using Birkeland (1984).
[c] Estimated by gravimetry.

Table II. Water balance for Lutz Creek Catchment

Year	P (m)	R (m)	Estimated PE (mm)[a]	Observed PE (m)[b]	Observed storage/loss (m)	Percentage observed storage/loss	Estimated storage/loss (m)	Percentage estimated storage/loss
1994	2·3	0·9	1·2	1·4	0·03	1·51	0·28	12·2
1995	2·5	0·9	1·2	1·4	0·28	11·48	0·46	18·2
1996	3·2	1·7	1·1	1·1	0·37	11·47	0·33	10·2
1997	1·7	0·4	1·2	1·4	0·01	−5·86	0·04	2·4
Average	2·4	1·0	1·2	1·3	0·15	6·09	0·28	11·4

[a] Based on the Penman–Monteith formula in Dietrich *et al*. (1982).
[b] Based on atmometer readings.

atmometer PE for this period was 11% higher than that estimated from the Penman–Monteith PE. Thus relative to the atmometer data, the Penman–Monteith estimates give a lower cumulative value of PE.

The assumption of a watertight basin may not be reasonable for Lutz Creek Catchment. If PE measured from canopy atmometer is used in a water balance (Table II), then 6% of annual rainfall is not accounted for by combined PE and runoff. Potential evaporation provides a liberal estimate of evapotranspiration because there are periods of the year when actual evapotranspiration (AE) does not equal PE (Dietrich *et al*., 1982). Therefore, the total amount of water unaccounted for in the water balance is probably greater than 6%. Some of the missing water enters groundwater storage because water can be observed emerging from seeps in calcic bedrock within and downstream from the catchment. It is unclear therefore, on a catchment scale, how much water is being extracted by the canopy species that have deep roots and how much is bypassing the weir as groundwater flow. Thus, a major ambiguity in our modelling is the relative balance between groundwater leakage and evapotranspiration in Lutz Creek Catchment and whether these processes can be differentiated.

Average hourly solar radiation from 1983 to 1998 approximates a semi-sinusoidal curve that begins roughly at 0700 hours, peaks at noon and goes to 0 at around 1900 hours (Figure 4). Wind velocity, a secondary factor in evapotranspiration, also follows a similar pattern but peaks at 1300. Because these two factors driving the daily cycle of ET follow a semi-sinusoidal path, a semi-sinusoidal representation is adopted here to distribute daily evapotranspiration totals to the 15-min time-steps that are used in modelling.

TOPMODEL modelling

The physically based hydrological model, TOPMODEL (Beven and Kirkby, 1979, Wolock, 1993, Beven *et al*., 1995a,b) was selected for this study because of its relative simplicity and limited data requirements. The model consists of linear and exponential equations that are solved quickly and directly. Model efficiency allows a large number of simulations to be run, so a broad range of physical conditions can be explored. Notably, topography is distilled into a single topographic index, discussed below, that can serve as a first-order surrogate for the distribution of soil moisture. The required input data include a DEM of the study area and time-series of precipitation and modelled evapotranspiration. Observed discharge is typically used to evaluate model efficacy.

TOPMODEL, with its statistical–dynamic structure, represents a compromise between detailed numerical models and statistical models of hillslope runoff. It also can help provide insight into the physics of catchment response and can be adapted easily for hypothesis testing (Piñol *et al*., 1997). Despite its physical basis, it is unclear the degree to which TOPMODEL parameters represent physically meaningful catchment characteristics. For example, the TOPMODEL transmissivity parameter, T_0, provides a closer approximation of plot-scale transmissivities than upscaled core measurements in Borneo (Chappell *et al*., 1998). However, the optimum calibrated value of T_0 has been shown to be dependent on the DEM grid-scale used for model input (Franchini *et al*., 1996; Saulnier *et al*., 1997). In the humid tropics, Molicova *et al*. (1997), Chappell *et al*. (1998) and Campling *et al*. (2002) utilized TOPMODEL to help determine the relative contributions of different flow paths in storm response but not to examine the water balance over seasonal or inter-annual periods.

The version of TOPMODEL used in this study has the following fundamental assumptions: (i) groundwater flow is steady state, (ii) the soil hydraulic conductivity decreases exponentially with depth, (iii) Darcy's Law is obeyed, and (iv) the hydraulic gradient parallels topography. The exponential profile provides a more rapid

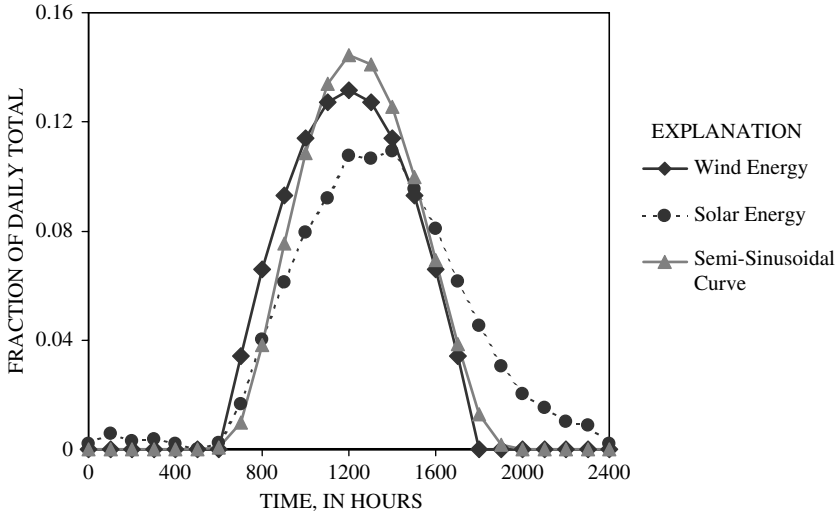

Figure 4. Average hourly distribution of wind and solar energy averaged from 1983 to 1998. Values are expressed as a fraction of the daily totals. A semi-sinusoidal curve from 0600 to 1800 hours is included for reference

decrease in transmissivity with depth than a linear, parabolic or power law profile (Ambroise *et al*., 1996; Igorulescu and Musy, 1997), so it was selected for the study. The steady-state assumption, which allows for model simplification, may be the most tenuous over short time-steps, because it takes a time proportional to upslope area for the water table to come to a steady state (Kirkby, 1997). The shortest time-step used in this modelling is 15 min, rather than the 5-min sampling time-step, in an attempt to reduce the number of time-steps used in modelling.

Beven and Kirkby (1979), Wolock (1993) and Beven *et al*. (1995a) present TOPMODEL derivations, so only a few model details are included here. The Fortran version TMOD9502, distributed by Lancaster University, was used (Beven *et al*., 1995b). The structure of the Lancaster model was modified as described below and the model parameters used in these simulations are described in Table III.

Model equations

The local saturation deficit, or the local depth to the perched water table multiplied by porosity, is generated from assumptions (1–4) listed above and is

$$S = S_{\text{avg}} + m\left(\gamma - \ln\left(\frac{a}{\tan\beta}\right)\right) \tag{1}$$

where S_{avg} (m) is the average saturation deficit or product of the depth to the water table multiplied by the porosity; m (m) is a scaling parameter that corresponds to the decrease in transmissivity with depth; $\ln(a\tan(\beta)^{-1})$, also referred to as the topographic index, is the natural logarithm of the ratio of upslope contributing area per contour length, a, to slope, tan (β); γ is the catchment average of $\ln(a\tan(\beta)^{-1})$. A local saturation deficit of 0 indicates that the soil is fully saturated and is therefore a source area for saturation overland flow.

The topographic index reflects the likelihood of saturation as affected by topography in a catchment with homogeneous soils. Areas with low values of the topographic index generally are divergent, steep slopes,

Table III. Description of model parameters that includes units, ranges used in Monte Carlo simulations and the mean value of 'accepted' results from basic model and direct flow model runs

Parameter	Description	Units	Monte Carlo parameter ranges		Mean 'Accepted' results	
			Minimum	Maximum	DF	Basic
Ln (T_0)	Transmissivity of saturated soil	ln(m^2/h)	−3	4	−0·79	−1·93
m	Controls the rate of decline of T_0 with depth	m	0	0·03	0·02	0·02
T_{d}	Controls the rate that recharge is added to the saturated zone per unit saturation deficit	h/m	0·001	50	24·5	22·3
RV	Constant stream routing velocity	m/h	500	5000	2798·2	810·0
$S_{\text{r}_{\max}}$	Maximum root zone deficit; controls the rate of actual ET	m	0	0·5	0·16	0·25
S_{r_0}	Initial soil moisture deficit	m	0	0·5	0·08	0·13
C_{LK}	Controls the rate of leakage from perched water table	m/h	$4{\cdot}00 \times 10^{-5}$	$2{\cdot}00 \times 10^{-4}$	$1{\cdot}22 \times 10^{-4}$	$1{\cdot}14 \times 10^{-4}$
F_{df}	Controls the percentage of recharge that becomes direct flow	None	0	0·6	0·27	0·00
$SD_{\max}$	Maximum mean saturation deficit, in excess of there is no groundwater leakage	m	0·2	0·5	0·35	0·35

have small contributing areas, are near ridges, and are least likely to be saturated. Areas with high values of the topographic index are convergent areas associated with valley bottoms and stream banks and are most likely to be saturated. Catchment cells with the same value of the topographic index have the same model water-table depth and perform identically in model calculations. Thus, instead of running the models for each catchment grid cell, maps of the topographic index are summarized as histograms that are used in model calculations (Figure 5) (Beven *et al*., 1995a). The $\ln(a \tan(\beta)^{-1})$ index necessary for TOPMODEL simulations was computed with the 5-m DEM derived in this study and a multidirectional flow algorithm (Wolock and McCabe, 1995).

The equation for catchment baseflow includes the scaling parameter, m, and attempts to express the relationship between average storage deficit, S, and subsurface flow

$$r_b = e^{-\lambda - \frac{S_{avg}}{m}} \tag{2}$$

where r_b (m/h) is unit baseflow and λ is the catchment average of $\ln(a\ T_0{}^{-1} \tan(\beta)^{-1})$; T_0 is the catchment average soil transmissivity (m^2/h) (Beven *et al*., 1995a). The expression indicates that as average storage deficit, S, decreases, baseflow increases exponentially, with a rate of recession determined by the value of m and T_0. For lack of better data and for simplicity, soil transmissivity is assumed to be spatially constant.

The recession constant m can be determined through hydrograph analysis. If recession periods are plotted with $\log(R)$ on the y axis and time on the x axis, the inverse of the slope is m (Beven *et al*., 1995a). We

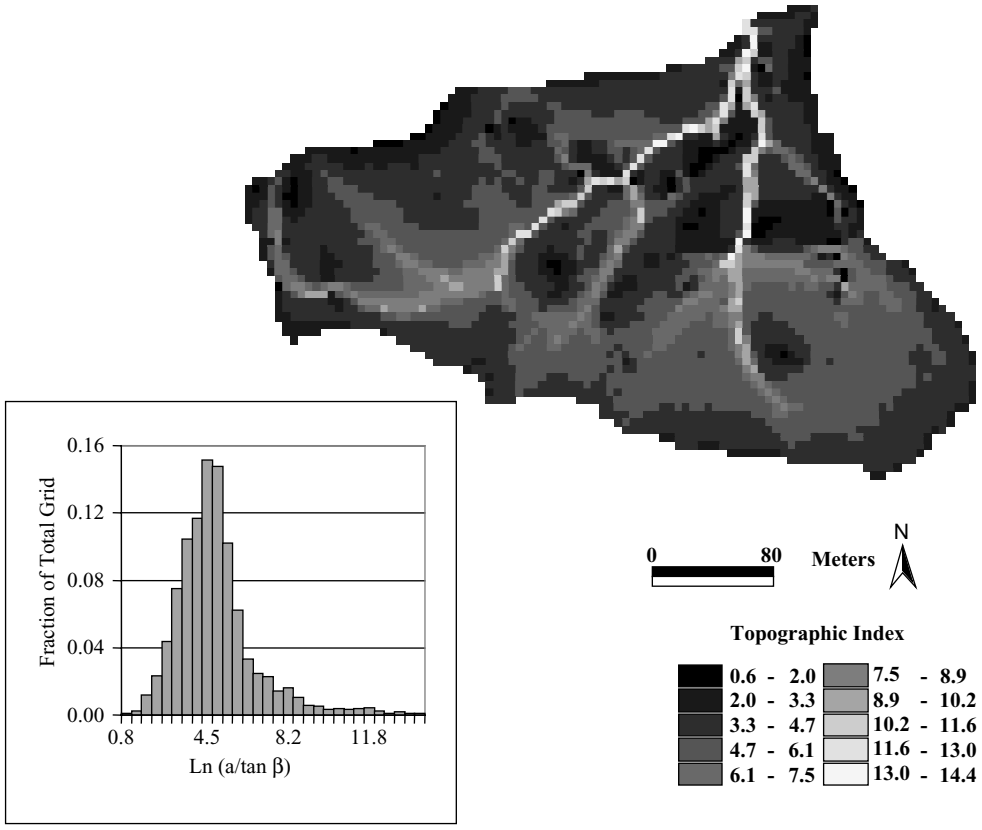

Figure 5. Map of $\ln(a \tan(\beta)^{-1})$ for Lutz Creek Catchment with $\ln(a \tan(\beta)^{-1})$ distribution used in modelling

examined all recession periods with more than 100 time-steps, and the maximum value of m was 0·03 m. Typically, recession constants during the wet season are 0·01–0·03 m.

Moisture in the root zone and evaporative efficiency are controlled in TOPMODEL by the expression

$$e_a = e_p \left(1 - \frac{S_r}{S_{r_{max}}}\right) \tag{3}$$

where S_r is the root-zone deficit, $S_{r_{max}}$ is the maximum root zone deficit, e_a is the actual root zone evapotranspiration (m/h) and e_p is the potential root zone evapotranspiration (m/h). The structure of Equation (3) suggests that as the moisture deficit increases, there is less water available to be evaporated and the disparity between AE and PE increases. This equation effectively includes evaporation from the canopy surface, as that process is similar to evapotranspiration from the soil (Rutter *et al*., 1975; Franchini *et al*., 1996).

The root-zone deficit is equivalent to the unfilled soil field capacity; it must equal zero (the root zone is full) before passing moisture through the soil. Once $S_r = 0$, then water conducted to the saturated zone is computed by

$$r_{uz} = \frac{S_{uz}}{S \times T_d} \tag{4}$$

where S_{uz} is the infiltrating moisture in excess of the field capacity ($S_r = 0$) and T_d (h/m) is a time delay parameter. This expression suggests that flow into the saturated zone, r_{uz} (m/h), decreases as the saturation deficit increases. The water represented by r_{uz} is then passed to the saturation zone where it then reduces S.

The basic version of TOPMODEL ignores pipeflow, which is an important flow component in some tropical catchments. A model representation for pipeflow and other fast flow-paths was added to TOPMODEL as 'direct flow', a mechanism that routes water to the stream without fully saturating the soil (Piñol *et al*., 1997). This algorithm originally was intended to route macropore and translatory flow in Mediterranean catchments.

The equation for direct flow from Piñol *et al*. (1997) is

$$r_{df} = r_{uz} \times F_{df} \tag{5}$$

where r_{df} is direct flow (m/h) and F_{df} is the fraction of water that flows through direct-flow pathways to the stream channel. The direct-flow algorithm is consistent with the observations of Uchida *et al*. (1999), who indicated that total pipeflow can be linearly related to total rainfall, and peak rainfall intensity can be related to peak pipeflow as well. Because water is routed through the unsaturated zone, the direct-flow algorithm delays the arrival of water at the stream relative to near-stream, saturation overland flow but delivers water more rapidly than throughflow. This timing is consistent with pipeflow response characteristics in some catchments (Jones, 1997). Comparison of basic and direct-flow versions of TOPMODEL may provide a test of the importance of pipeflow or another delayed near-surface stormflow source.

Both the direct-flow and basic models account for macroporosity. In the case of the basic model, macroporosity is implicitly considered by maximizing transmissivity at the surface of the soil through an exponentially decreasing permeability distribution with depth. For the direct-flow model, this linear expression for macroporosity is superimposed on the exponential transmissivity distribution.

For Lutz Creek Catchment, we assume that there may be significant losses to groundwater, so it was necessary to modify TMOD9502 further. For groundwater loss, the following equation was used

$$l_g = C_{LK} \left(1 - \frac{S}{Sd_{max}}\right) \tag{6}$$

where l_g is the groundwater leakage per unit area into the bedrock, C_{LK} is a loss constant (m/h) and S_{max} (m) is the maximum deficit that allows leakage. If the mean saturation deficit exceeds S_{max}, then deep groundwater loss ceases. The equation for groundwater loss is similar to a groundwater-loss equation of Leavesley *et al*.

(1983) if a first-order power law is assumed in their equation. This expression indicates that as the saturation deficit is reduced, the corresponding increase in pressure at the base of the water table forces water into the regolith.

At the conclusion of each time-step, the mean saturation deficit is updated by using the following mass balance equation that includes deep groundwater losses

$$S_{\mathrm{avg}_t} = S_{\mathrm{avg}_{t-1}} + (r_b + l_g - r_{uz}) \times \mathrm{d}t \tag{7}$$

where S_{avg_t} is the current mean saturation deficit and $S_{\mathrm{avg}_{t-1}}$ refers to the deficit of the preceding time-step.

Chemical constraints

The use of solute chemistry provides additional constraints to TOPMODEL by tagging flow paths. A mix of physically based and end-member-mixing models was used to examine the partitioning of water among various pathways: evapotranspiration, overland flow, macropore flow, subsurface matrix and deep groundwater. The aim is to differentiate overland, macropore and subsurface-matrix flows in TOPMODEL using solute chemistry for cross-validation. This approach is similar to that of Guntner *et al*. (1999)

Natural chemical tracers provide a potent method of assessing flow paths in smaller watersheds. Two principles are involved. One is the assumption that chemical mass balances smooth out small-scale variability within the watershed, producing an integrated signal. The second is that waters from different vertical hydrological compartments within a watershed have distinctive chemical signatures. Accordingly, these distinctive chemical sources are referred to as mixing end-members. Because there is little evidence for spatial variability in end-member chemical signatures, only vertical variations in end-member compositions are considered here.

End-member mixing models are often used to separate hydrographs into their flow-path components (i.e. Christophersen *et al*., 1990; Hooper *et al*., 1990; Rice and Hornberger, 1998). Ideally, the natural tracers cannot participate in chemical reactions, and sources must have unique chemical signatures and concentrations that are temporally invariant (Rice and Hornberger, 1998). These requirements are fundamentally at odds with the reality that biogeochemical processes create the chemical signatures. End-member-mixing models are appropriate where hydrological mass transport is rapid compared with the rates of biogeochemical processes that make the signatures and where end-member reservoirs are not depleted in solutes by sustained flows. Even under ideal conditions, Rice and Hornberger (1998) demonstrated that different tracers may generate disparate descriptions of storm flow separation. Hysteresis in the chemical signature for the rising and falling limbs of the hydrograph, perhaps caused by solute depletion, can also add complexity to using chemical end-members to distinguish flow paths (Scanlon *et al*., 2001).

Studies have integrated chemical mixing models with TOPMODEL in order to understand the temporal variability of acid neutralizing capacity (alkalinity) (Robson *et al*., 1992), DOC concentrations (Hornberger *et al*., 1994; Boyer *et al*., 2000) and silica concentrations (Scanlon *et al*., 2001) in stream water. These studies have used TOPMODEL to predict the amount of water derived from various depths of the soil that have specific chemical signatures. Guntner *et al*. (1999) used chemical mixing predictions as one of many TOPMODEL validation criteria.

Modelling approach and hypothesis testing

Piñol *et al*. (1997) used TOPMODEL to test hypotheses about the hydrology of Mediterranean catchments by devising six different model structures. Examples of different model structures included varying the root-zone depth with the topographic index and adding the direct-flow (macropore) term described by Equation (5). They then tested the different model structures to determine which provided the best representation of catchment hydrology, suggesting which of their perceptual models best described catchment hydrology.

In Lutz Creek Catchment, a similar approach is applied by testing three models: (i) a basic model, which is TMOD9502, run on a 15 min time-step, with the addition of groundwater leakage; (ii) the basic model plus

groundwater leakage and the direct-flow expression from Piñol *et al*. (1997), which is also run on a 15 min time-step; (iii) the same direct-flow model run on a daily time-step. The time-series used in modelling is an 8-year time-series from 1990–1997. The first year is not included in either the hydrograph fit or water balance calculations in order to remove the effect of initial conditions. Nevertheless, chemistry data over the entire 1990–1997 period are used in our model evaluation because removing these data would leave us with a limited number of samples to evaluate our simulations.

The direct-flow term is added to test whether processes such as the observed pipeflow may be important fast pathways in Lutz Creek Catchment. If the catchment responds like other Acrisol catchments, this term may be necessary to represent dynamics not included in the original version of TOPMODEL. The direct-flow model was run on a daily time-step to compare how well the model performed on the 15-min and daily time-steps.

Monte Carlo analysis

We used a Monte Carlo-based calibration method to run TOPMODEL. This assigns parameter set likelihoods using an approach similar to the general likelihood uncertainty estimation (GLUE) of Beven and Binley (1992) and Freer *et al*. (1996). For all versions of the model, 8000 TOPMODEL simulations were run for a 7-year interval with parameters chosen randomly from a physically reasonable suite of parameter distributions. By completing many runs, uncertainties owing to equifinality, the property that many parameter sets can produce equally reasonable results, can be addressed (Beven, 1993). Equifinality in this system can be attributed to measurement errors of model inputs, changing hydrological conditions over time, non-linearities in hydrological response, or model structural deficiencies.

Each simulation was evaluated based on the goodness of fit between observed and simulated hydrographs as computed using the Nash–Sutcliffe efficiency statistic

$$E = 1 - \frac{{\sigma_r}^2}{{\sigma_o}^2} \tag{8}$$

where ${\sigma_r}^2$ is the variance of the residuals between the observed and simulated hydrographs and ${\sigma_o}^2$ is the variance in the observed discharge. An efficiency of 1 implies a perfect fit between observed and simulated data; negative efficiencies indicate a poor fit. Because efficiencies include a sum of squares of the differences, efficiency would appear to be biased towards the successful matching of peak flows. However, the length of interstorm periods in the hydrological record also requires that they are matched reasonably well to obtain high efficiencies. Periods of missing or zero discharge measurements are not included in the efficiency calculations, thereby excluding 280 days over the 7-year time-series.

Once efficiencies are calculated, a likelihood can be assigned to each of the parameter sets. Here, a modification of the GLUE procedure is adopted. Because of differences in efficiencies among model versions, instead of defining an arbitrary threshold of efficiency, the top 10% of results ranked by efficiency for all models are taken. Efficiencies below the top 10% ranking are discarded, effectively receiving a likelihood of zero (Freer *et al*., 1996). Efficiencies above the threshold value are considered 'accepted' ('behavioural' according to the terminology of Beven and Binley (1992) and Freer *et al*., (1996)) and were converted to a likelihood using the following equation

$$l = \frac{E_i}{\sum_{i=1}^{n} E_i} \tag{9}$$

where l is a likelihood, E is efficiency and n is the number of parameter sets above the threshold efficiency value. The likelihoods are updated using goodness of fit with the chemical mixing model that is described below.

End-member chemical mixing

Chemical constraints were provided by assigning a chemical signature to relevant mixing end-members and comparing the observed stream composition to the model-predicted composition. Dry-season samples are excluded in establishing end-members. Under extreme low-discharge conditions, the channel above the pool at Lutz weir has no discharge, and the pool is presumably spring-fed at a very low rate. Because of a deep source of water, the composition of the water becomes aberrant at that time.

For wet season samples the concentrations of Na^+, Mg^{2+} Ca^{2+} and Cl^- are highly positively correlated (Figure 6). Only K^+, which is negatively correlated with the other solutes, increases with increasing flow. $Si(OH)_4$ is anomalous, with some storms showing an increase with discharge and others showing a decrease. For Lutz Creek, a *Q*-mode factor analysis (Stallard and Edmond, 1983) with the constituents Ca^{2+}, Cl^-, K^+, Mg^{2+}, Na^+, $NO_3{}^{2-}$, $PO_4{}^{2-}Si(OH)_4$ and SO_4 suggests that 97% of the variance in measured constituents ($n = 55$) can be explained by three end-members and 95% of the variance is explained by only two end-members.

Figure 7 shows a ternary diagram with the end-members labelled by the chemical constituent that is especially concentrated in that end-member. Most of the data lie on the axis between and end-member rich in bedrock constituents and one rich in K+ and $NO_3{}^{2-}$. It therefore appears that the wet season chemistry can be defined by two end-member compositions: a surface end-member with low concentrations of major constituents (except K^+) and a subsurface end-member with high concentrations of major constituents.

The mass-balance relationship for two-component mixing can be expressed in the following form

$$C_t = C_s + (C_b - C_s)\frac{r_b}{r_t} \tag{10}$$

where C_t, C_s and C_b are the total, surface flow and saturated subsurface concentrations of a solute and r_t and r_b are the specific stream discharge and specific subsurface discharge (baseflow) respectively: C_t is the observed concentration in stream water, and r_b/r_t is the independent variable obtained from TOPMODEL

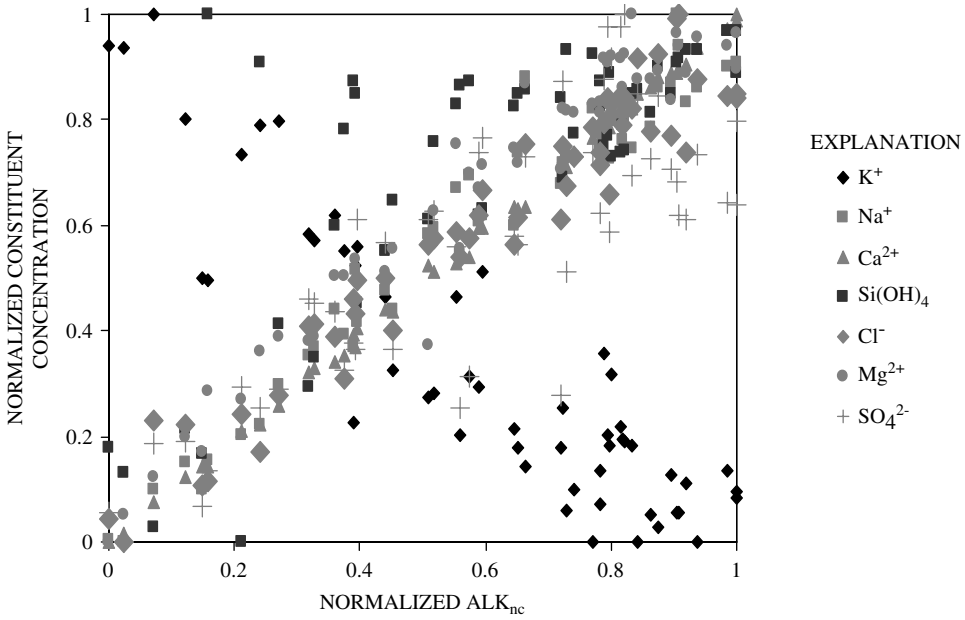

Figure 6. Comparison of various constituents with the synthetic constituent bedrock alkalinity (defined by Equation 12). All constituents are normalized by the sample range (0–1)

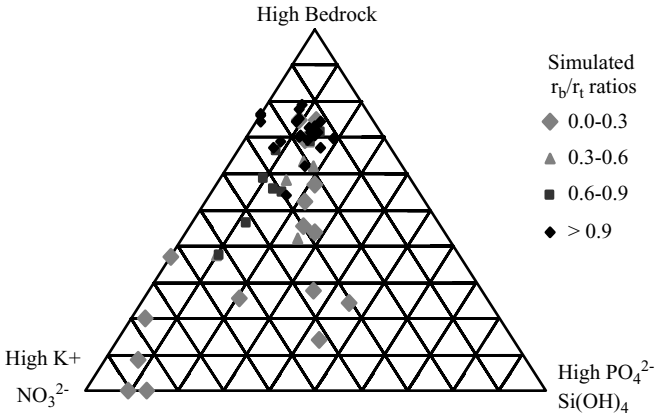

Figure 7. Ternary diagram showing the position of wet season chemical samples relative to three end-members calculated through Q-mode factor analysis. Samples are labeled by r_b/r_t ratios from the best-fit direct-flow run

simulations. A linear regression between the C_t of a given constituent and r_b/r_t from Equation (10) provides a measure of goodness of fit (in terms of r^2) between chemistry and TOPMODEL results. It also predicts the concentrations of C_s from the intercept and the quantity $(C_b - C_s)$ from the slope. These concentrations can be used later to compute overall annual fluxes for a catchment if yearly totals of r_b and r_s are specified.

This procedure deviates from the end-member mixing analysis (EMMA) often pursued in the literature. The conceptual model of chemical mixing used is based on factor analysis (e.g. Stallard and Edmond, 1983; Stallard *et al.*, 1991) and knowledge of catchment chemistry rather than using the observed chemistry of end-members measured in lysimeters. This methodological choice is the result of insufficient field measurements. The geological heterogeneity of Lutz Creek Catchment probably precludes an ability to define each end-member through sampling a small number of sites (e.g. Litaor, 1988). Given the small area of Lutz Creek Catchment, it is assumed here, despite the geological variability, that the end-member signatures averaged over the catchment for each storm are similar.

In a water sample with a pH less than 9, in which the ions of the carbonate system [H^+, OH^-, HCO_3^-, CO_3^{2-}] dominate over other weak ions, as is the case for all samples from Lutz Creek, then alkalinity is simply the difference between the non-acid-titratable cations and the non-acid-titratable anions (Morel, 1983, pp. 134–136). If the non-acid-titratable ions are conservative, then alkalinity is conservative. The concentrations of nitrate and ammonia are large and variable in Lutz Creek samples, perhaps owing to active uptake on flow paths, riparian processes and tapir faeces. Accordingly, a nitrogen-corrected alkalinity was defined to remove the gains and losses of ammonia and nitrate as water moves through soils and riparian zones

$$\mathrm{alk_{nc}} = [\mathrm{Na^+}] + [\mathrm{K^+}] + 2[\mathrm{Mg^{2+}}] + 2[\mathrm{Ca^{2+}}] + 2[\mathrm{Sr^{2+}}] - [\mathrm{Cl^-}] - 2[\mathrm{SO_4^{2-}}] \quad (11)$$

Ca^{2+} and Mg^{2+} dominate the alk_{nc} because of the weathering of the carbonates and volcaniclastics in the catchment. Sea-salt blown inland contributes considerable Na^+, Mg^{2+}, Cl^- and SO_4^{2-}, but relatively little negative alkalinity. Thus, nitrogen-corrected alkalinity represents the entirety of bedrock-derived ionic inputs, and therefore should be fairly conservative.

Instead of using end-members derived statistically from the Q-mode factor analysis, alk_{nc} was chosen for use in Equation (10). In the Lutz Creek system, any number of end-members could be selected because the major ion, non-nutrient constituents are highly correlated. The alk_{nc} represents movement along the left axis of the ternary diagram in Figure 7 and is a physically based rather than statistically derived parameter.

Surface-water components, C_s and Q_s, are defined differently for each of the modelling approaches. In the case of the basic model (model 1), surface water comprises only overland flow. When the direct model is

used (models 2 and 3), the surface water is both overland flow and other 'direct flow'. As Elsenbeer *et al.* (1995) found at La Cuenca, Peru, overland flow and macropore flow frequently intermingle and have a similar K^+-rich composition.

After the r^2 between alk_{nc} and r_b/r_t ratios is computed, chemical likelihoods are calculated using Equation (8) by replacing efficiency with the r^2 values. The total likelihood measure—a combination of fit to alkalinity and the hydrograph—is then calculated by multiplying the chemical likelihood and efficiency likelihood.

RESULTS AND DISCUSSION

Comparison of direct-flow and basic models

For the purpose of this discussion, the 'accepted' Monte Carlo results for 15-min scale simulations are defined as those parameter sets that meet the following criteria: (i) top 10% by efficiency and (ii) top 10% of r^2 fits when r_b/r_t ratios are compared with chemistry through a regression on Equation (10). The most likely single result is that with the greatest combined chemistry correlation and TOPMODEL efficiency likelihood.

The inclusion of the direct flow expression (Equation 4) improves results. If 'accepted' runs are compared (Figure 8), the direct-flow model both provides a better fit to the observed chemistry and generally also provides higher TOPMODEL efficiencies. At higher efficiencies, particularly for the basic model, the fit with the chemistry decreases. This phenomenon is indicative of the trade-off of matching peak flows (high efficiencies) and matching the recessions (high r^2 fit to chemistry).

The improvement in geochemical fit by using the direct model can be seen by comparing the r_b/r_t estimates from the best-fit basic, model 1, and the best-fit direct-flow, model 2, shown in Figure 9, a graph of r_b/r_t for the September 1990 storm. The observed r_b/r_t ratios are estimated by solving Equation (10) for each of the samples on 1 September 1990, using a C_s of 450 μeq/L (the lowest observed value for September 1990) and

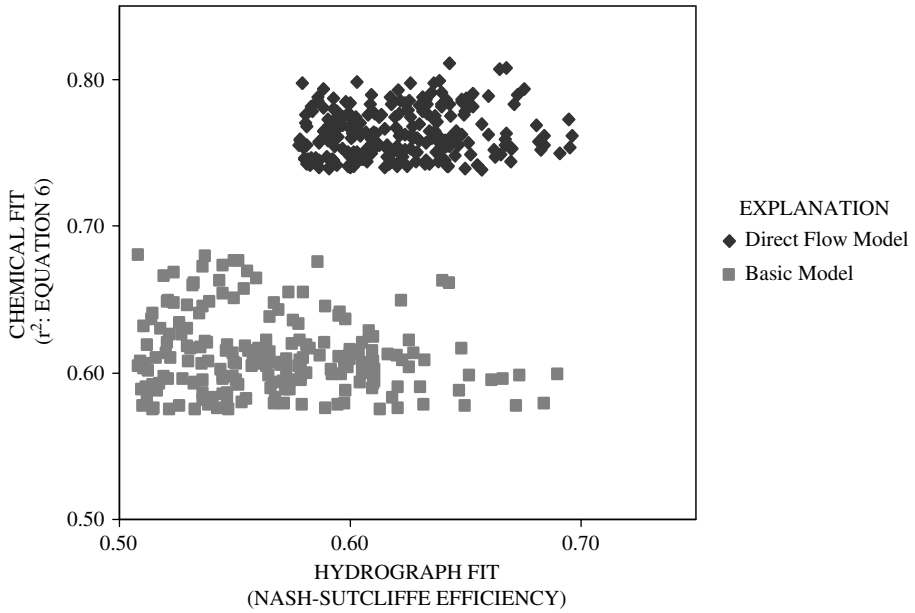

Figure 8. Comparison of Nash–Sutcliffe efficiencies and r^2 fit between bedrock alkalinity and r_b/r_t ratios (Equation 11) for 'accepted' direct flow and basic model simulations. Accepted simulations are defined as those runs ranked in both the top 10% of all runs as ranked by efficiency and the top 10% of all runs in chemical fit

a C_b of 3600 μeq/L (an average baseflow value for September 1990). The direct flow results provide a better fit to the estimated r_b/r_t because there is a delayed return to storm, baseflow conditions. This observation indicates that there is a surface contribution to the receding limb of the stream hydrograph, from a delayed surface or near-surface water source.

The basic model results also indicate that a greater subsurface delay is necessary to improve the modelled fit to the observed chemical data even without direct flow. Figure 10 shows the cumulative frequency distributions of three parameters in the basic version of TOPMODEL for efficiency as the likelihood criterion ($n = 800$) and for efficiency + chemistry as the likelihood criteria ($n = 234$). If one compares the 'accepted' parameter sets as determined by efficiency relative to those obtained by adding the chemistry data, it is clear that in order to match the stream chemistry, lower stream velocities (RV), lower soil transmissivities (T_0) and greater subsurface delays (T_d) are necessary. All of these shifts in parameterization favour the delayed arrival of surface or near-surface flow at the catchment outlet and increase the relative contribution of the quickflow component later in the hydrograph.

There are many reasonable interpretations of this delayed surface or near-surface water source, of which two are favoured here. One possible explanation is the abundant, observed soil pipe networks. Alternatively, these results could also indicate that saturation overland flow may be delayed, potentially because of its association with soil pipes (Elsenbeer and Vertessey, 2000). If peak runoff rates for Lutz Creek are superimposed on the storm flow diagram of Jones (1997), Lutz Catchment plots nearly on the border of the pipeflow and saturation overland flow fields (peak flows c 0·01 mm/0·09 km^2). The peak flows per watershed size are similar to La Cuenca, where Elsenbeer and Vertessey (2000) found that the coupling of overland flow and pipeflow made the two processes difficult to distinguish and that the lag times of both processes overlap. Without quantitative estimates of a pipe contribution that has been observed (S. Paton, 2002, personal communication), it is difficult to pinpoint the exact source of this delayed surface storm water in Lutz Creek Catchment.

Regardless of its exact interpretation, the direct-flow model allows for a rapid subsurface response without fully saturating the soil, and it is probably consistent with Lutz Creek catchment having an Acrisol-style runoff response. Delays in the arrival of a near-surface source could indicate that runoff is not derived in variable contributing areas adjacent to the stream but rather elsewhere in the catchment. The rapid response

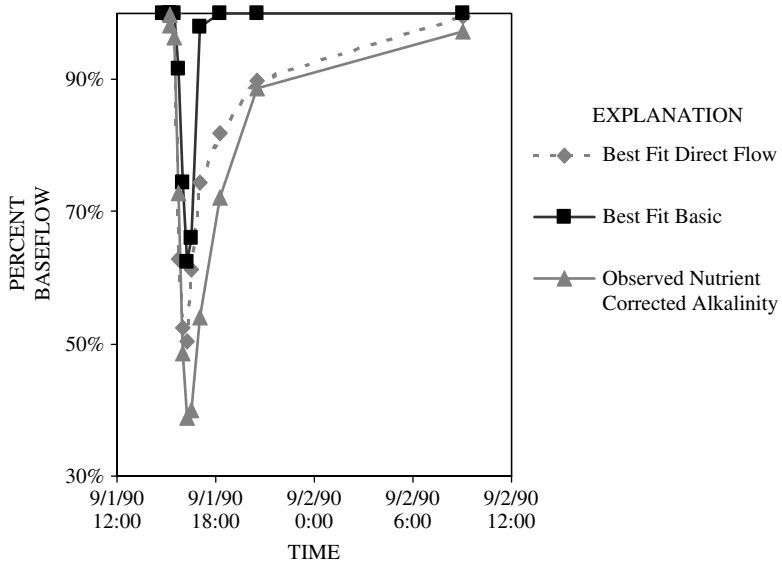

Figure 9. Comparison of three estimates of alk_{nc} during a 1 September 1990 storm. The three estimates are the best-fit basic model simulation, the best-fit direct-flow simulation and observed alk_{nc} during the storm

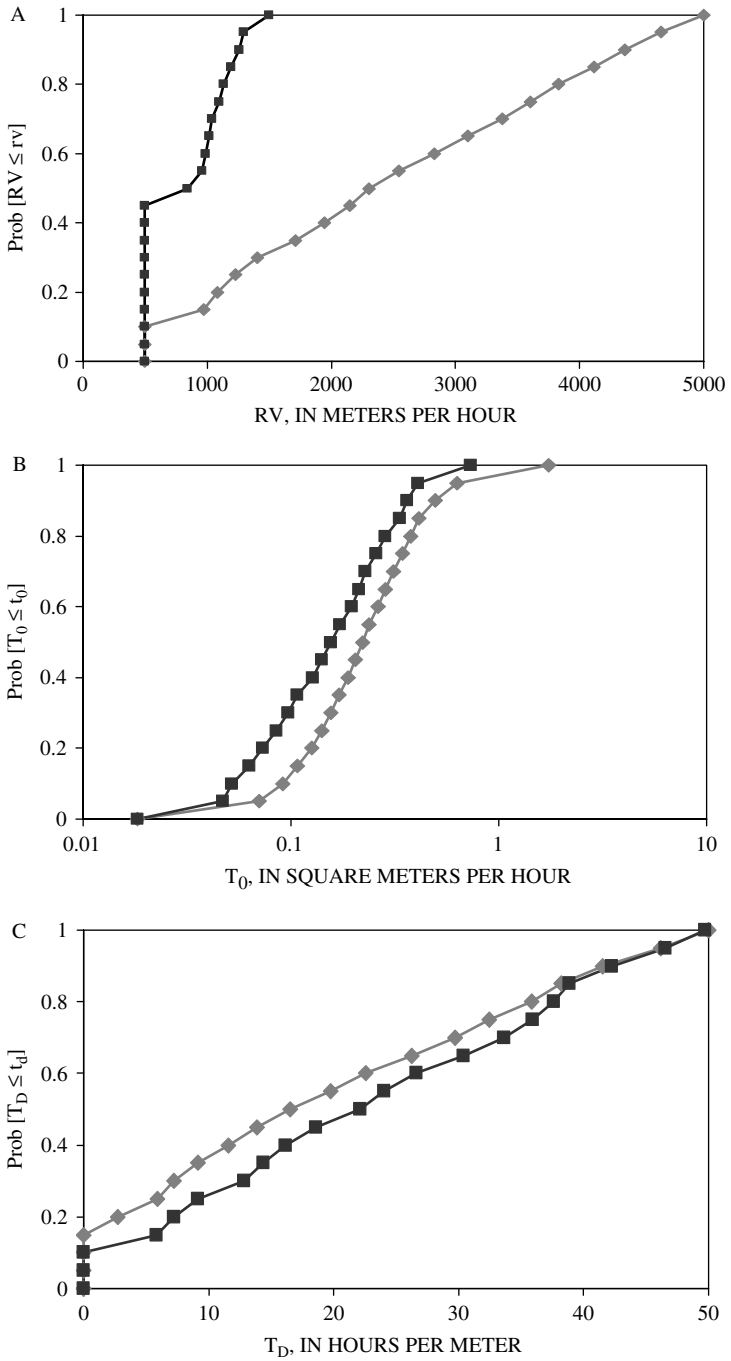

Figure 10. Cumulative frequency distributions of basic model 'accepted' runs for three TOPMODEL parameters: (A) *RV* (routing velocity), (B) T_0 (soil transmissivity), (C) T_D (delay constant). Two distributions are presented in each figure: ■ = 'accepted' runs using both Nash–Sutcliffe and chemical fit as rejection criteria, ◆ = 'accepted' runs if Nash–Sutcliffe is the only rejection criterion

afforded by the direct-flow model also may be compensating for a lack of transient dynamics in the steady-state formulation of TOPMODEL that we use. The combination of TOPMODEL and chemistry data, however, indicates the importance of a delayed surface or near-surface contribution that arrives at the weir well after the hydrograph peak.

The overall flow partitioning among water-transport pathways for the likelihood-weighted average of 'accepted' results is similar to that predicted by Dietrich *et al*. (1982) from hydrograph analysis. If the direct-flow model is used, then overland flow is 9·7% of total runoff for the 7-year period (Table IV). The overall total of 50% overland + direct flow is similar to the 51% quickflow + delayed flow estimated by Dietrich *et al*. (1982) using hydrograph-separation techniques.

Water balance results

The evapotranspiration term of the Lutz Creek water balance was difficult to quantify, and continued work will be necessary to improve this part of the model.

To increase evaporation in the catchment, we modified the size of the root zone. The maximum root zone deficit, $S_{r_{max}}$, is the moisture deficit between field capacity and wilting point. Using a 0·4-m-thick root zone (Dietrich *et al*., 1982), and a range of soil-moisture contents between 19 and 30% by volume (Kursar *et al*., 1995), we calculated the maximum root zone deficit to be $0{\cdot}4 \times (0{\cdot}30-0{\cdot}19)$ or 0·044 m. Because this is a rough estimate and does not include any canopy storage, a maximum upper value of 0·05 m was used initially in model calculations. Initial runs of models 1 and 2, based on this computed zone, had too little evapotranspiration and overestimated discharge by up to 150% per year. To increase evaporative efficiency, the maximum root zone size was allowed to be up to 0·5 m water equivalent, which is approximately 5 m of soil thickness. Water balance calculations were improved by increasing C_{LK} from $2{\cdot}0\ 10^{-5}$ to $2{\cdot}0\ 10^{-4}$ to provide for additional groundwater leakage. These changes in parameterization were successful in balancing the long-term water budget of the catchment. All of the parameter ranges used in Monte Carlo simulations are reported in Table III.

Despite the adjustments of parameter ranges, the water balance in Table V still has relatively low values for AE and relatively high values of groundwater loss. The increased losses could be compensating for an underestimation of evapotranspiration during the wet season, a situation that is clearly possible given our application of the Penman–Monteith formula. There are three possible inadequacies in our representation of evapotranspiration in the model: (i) not distinguishing interception from soil moisture, (ii) not accounting for deeper groundwater storage, and (iii) using the Dietrich *et al*. (1982) version of the Penman model.

The structure of the model aggregates both canopy storage and soil moisture storage. Modelling interception separately would essentially allow the system to evaporate at two different rates. Even if the soil were dry,

Table IV. The annual and overall division of flow through overland, direct-flow and overland-flow paths all expressed as a percentage of total runoff. The values were generated by a weighted average of 'accepted' results

Year	Basic model		Direct flow model		
	R_b	R_{of}	R_b	R_{df}	R_{of}
1991	78·9	21·1	49·1	42·5	8·4
1992	71·6	28·4	51·5	35·6	12·8
1993	76·6	23·4	51·1	39	9·9
1994	78·8	21·2	49·8	41·8	8·4
1995	80·4	19·6	45·9	46·6	7·5
1996	74·0	26·0	52·9	35·8	11·2
1997	84·9	15·1	37·7	57·4	4·9
Total	76·3	23·7	49·7	40·6	9·7
Average	77·9	22·1	48·3	42·7	9·0

Table V. An annual simulated water balance. These values are reported in metres of water and are obtained by averaging all 'accepted' runs for both the basic and direct flow model cases

Model	Year	R_1[a] (m)	R_2[b] (m)	AE (m)	Loss (m)	R_b[c] (m)	R_{df}[c] (m)	R_{of}[c] (m)	Store (m)	R_s/R_o[d]
Basic model	1991	0·85	0·85	0·99	0·65	0·67	0·00	0·18	−0·02	0·97
	1992	1·44	1·44	0·88	0·67	1·03	0·00	0·41	0·03	1·03
	1993	1·06	1·12	0·96	0·64	0·85	0·00	0·26	0·02	0·89
	1994	0·81	0·83	0·90	0·63	0·65	0·00	0·18	−0·07	1·09
	1995	0·74	0·74	0·98	0·64	0·60	0·00	0·15	0·12	0·93
	1996	1·12	1·54	1·02	0·73	1·14	0·00	0·40	−0·07	1·30
	1997	0·29	0·30	0·95	0·57	0·25	0·00	0·04	−0·09	0·90
	Total	6·31	6·82	6·68	4·53	5·20	0·00	1·62	−0·07	1·02
Direct flow model	1991	0·95	0·95	0·93	0·61	0·46	0·40	0·08	−0·01	1·08
	1992	1·53	1·53	0·82	0·64	0·79	0·54	0·20	0·03	1·10
	1993	1·15	1·20	0·92	0·60	0·61	0·47	0·12	0·02	0·96
	1994	0·88	0·91	0·85	0·59	0·45	0·38	0·08	−0·06	1·16
	1995	0·85	0·85	0·93	0·60	0·39	0·40	0·06	0·10	1·07
	1996	1·18	1·61	0·99	0·70	0·85	0·58	0·18	−0·06	0·99
	1997	0·40	0·41	0·89	0·52	0·15	0·23	0·02	−0·09	1·21
	Total	6·93	7·44	6·33	4·26	3·71	3·00	0·74	−0·07	1·08

[a] R_1 is total simulated flow during periods with corresponding observed discharge data.
[b] R_2 is the total simulated flow for the whole run.
[c] R_b, R_{df}, R_{of} are the yearly integrals of q_b, q_{df}, and q_{of}, respectively and have units of meters.
[d] R_s/R_o is the ratio of simulated to observed flows.

the canopy surface could be 'saturated' and evaporating at a higher rate than the soil. This would enhance the ability of the rainforest system to evaporate close to a rate for which AE = PE. Additionally, the factors that control interception, including storm size, direction and intensity, may change the ability of trees to intercept precipitation and timing of evapotranspiration. A layered evaporative model may address some of the inadequacies in the estimation of evapotranspiration.

Our implementation of the Penman equation also may be a factor in underestimating ET. As suggested earlier, PE measured by the atmometer was 11% higher than that estimated with the Penman equation of Dietrich *et al.*, (1982) for the years for which the two estimates overlapped. Another equation for PE implemented in concert with a canopy model may increase the overall contribution of PE in the water budget.

Trees may be removing water from what is deep groundwater in the model to increase ET. Under this scenario, water drains from surface soil during the wet season when moisture is readily available and enters a deeper, low-hydraulic conductivity zone. The water is then stored in the regolith when canopy trees, responding to drought, utilize it and convert it into water vapour. Hydraulic lift may also bring water to non-canopy plants during the dry season.

The increase in evaporative depth allowed plants to have a larger supply of moisture during dry season months may have represented the deep-rooting potential of trees. Both carbon isotope analyses (Sternberg *et al.*, 1989) and irrigation experiments (Wright and Cornejo, 1990) on BCI, indicated that many trees are not water-stressed during the dry season. Wright and Cornejo (1990) showed that leaf flush, leaf fall and flowering were affected in understory shrubs but not in deeper rooted trees. The trees therefore must have a deep source of soil water when near-surface stores of moisture are exhausted. This is consistent with our revised root-zone depth of 5 meters.

TOPMODEL and the daily time-step

To demonstrate the applicability of TOPMODEL to long-term ecological research, TOPMODEL was tested at a daily time-step. Concordant results would, for example, provide a tool for predicting the long-term moisture status of Lutz Creek Catchment, given a record of daily precipitation.

TOPMODEL provides a reasonable fit to observed stream flow on a daily time-step (Figure 11). There were several efficiencies in excess of 0·9 and over 8% of the 8000 Monte Carlo runs had efficiencies greater than 0·8. Clearly, TOPMODEL provides a better match to daily discharge totals than it does at a shorter time-step in which it has to match the dynamics of individual storms.

Another important aspect of daily TOPMODEL runs is that they provide similar cumulative flow separation estimates to the runs on a 15-min time-step. To illustrate this, the total water deficit is defined as $S_r + S$. Then, a linear regression is used to obtain the explained variance (r^2) measured fit between observed and simulated soil moisture. Daily 'accepted' runs were defined as those that are both in the top 10% by efficiency for daily discharge and in the top 10% r^2 fit for biweekly average observed soil moisture. The daily and 15-min results for daily 'accepted' parameter sets are plotted in Figure 12. As indicated in Figure 12, for direct flow and baseflow, there is nearly a 1-to-1 correspondence between daily and 15-min totals. However, predicted overland flow at the 15-min step is 73% of that calculated using the daily time-step.

The similarity between 15-min and daily results reflects the way temporal dynamics of important processes are implemented in TOPMODEL. Direct flow, as indicated in Equation (5), is simply a proportion of total recharge or the excess of soil field capacity, R_{uz}. As R_{uz} should be nearly identical at either time-step, R_{df} also should be similar. Conversely, saturation overland flow is less at the 15-min time-step because of model dynamics. For the daily time-step, the addition of all of the water at once leads to immediate saturation of areas of high $\ln(A/\tan\beta)$. Conversely, the 15-min time-step saturates these regions later in the storm. There are therefore fewer saturated source areas at the 15-min time-step, reducing the amount of saturation overland flow. As the direct flow component delivers more water than saturation-excess overland flow, the totals for each flow path are similar for either the 15-min or daily time-step.

At a daily time-step, TOPMODEL provides a reasonable approximation of observed soil moisture (Figure 13). In regressions between observed available water and simulated total deficit for the same parameter sets examined in Figure 11, 93% of the simulations had r^2 values greater than 0·7. If one examines a simple regression model comparing rainfall from a varying number of preceding weeks, representing antecedent conditions, with observed biweekly soil moisture, the best-fit occurs if rainfall from the previous six weeks is used and the r^2 is only 0·68. Therefore, it appears that TOPMODEL improves soil moisture prediction over simple regression models of antecedent rainfall.

CONCLUSION

We hypothesized that a hydrological model with only subsurface and saturation overland flow routing, as formulated in TOPMODEL, would be sufficient to model the dynamics of Lutz Creek Catchment. Although this basic version of TOPMODEL provides reasonable results, models with the linear direct-flow term of

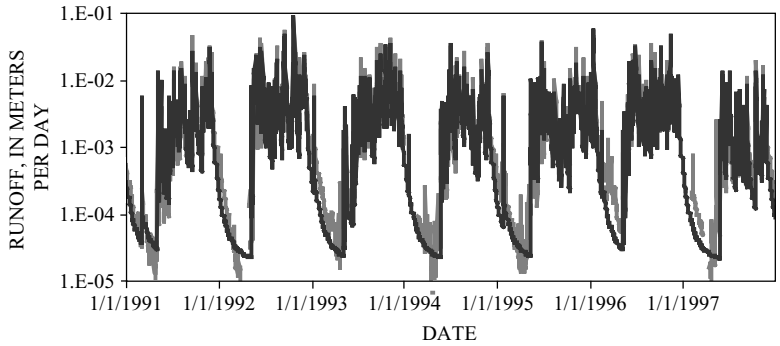

Figure 11. A comparison of observed (thick grey line) and simulated (thin black line) daily runoff for the years 1991–1997. This model run was the best-fit of all daily direct flow runs

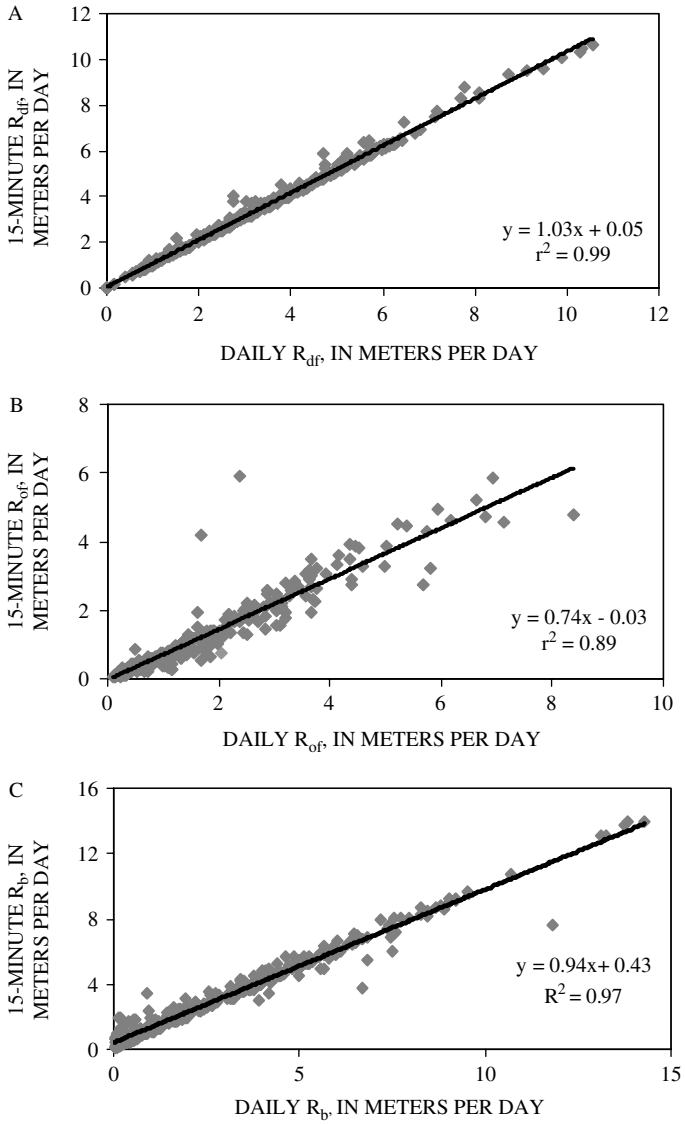

Figure 12. A comparison of daily and 15-min water balance estimates for direct-flow parameter set realizations that are in the top 10% of efficiency for daily discharge and in the top 10% of r^2 fit between observed and simulated soil moisture. The graphs are of (A) direct flow, (B) overland flow and (C) baseflow. Regression equations and r^2 fits are included for reference

Piñol *et al*. (1997) outperform it. This suggests that a delayed source such as the observed pipe networks, a delayed saturation overland flow component, or a combination of the two may play a primary role in fast flow routing in Lutz Creek Catchment. Both 15-min and daily models work well, indicating that TOPMODEL can be reasonably applied to long-term daily rainfall–runoff data sets. The weakness of the implemented model is the balance between evapotranspiration and groundwater losses.

As in other tropical catchments, high K^+ and low alkalinity concentrations during the wet season define fast-flow routing. Modelling results indicate that these flowpaths contribute around 50% of the total flow over the 7-year period. This estimate agrees favourably with Dietrich *et al*.'s (1982) hydrograph separation, where they analysed 51% of the flow to be quickflow and delayed flow.

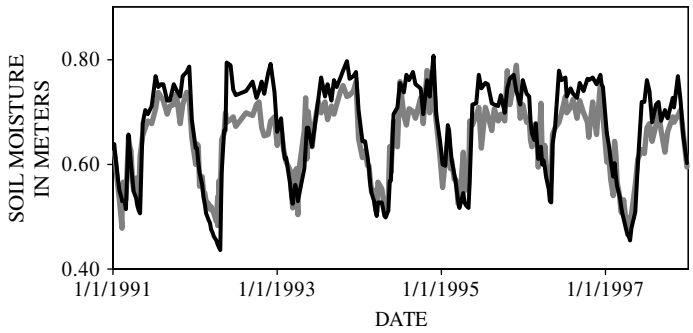

Figure 13. Example of a model run (thin black line) of soil moisture for 1991–1997 (as total available moisture in m) for the best-fit daily direct flow run. Field data (thin grey line) were converted to total moisture from weight per cent water content recorded biweekly at 0 to 0·2 m and 0·2 to 0·4m soil depths. To create this graph: (i) TOPMODEL root-zone and soil saturation deficits are summed to obtain a total deficit, (ii) available water capacity (AWC) and bulk density as given by Windsor (1990) were used to calculate total moisture from observed gravimetric estimates, and (iii) the beginning of the model output and the observed data were adjusted to match

Other field observations, independent of TOPMODEL, are needed to validate evaporative and groundwater loss fluxes. Although the water budget has been balanced by increasing groundwater loss, it is unclear whether these losses are real. It is important that future work focuses on the timing of PE relative to moisture availability instead of simply assuming AE is equivalent PE. TOPMODEL provides a constraint by suggesting that there needs to be more moisture available to evaporate during the dry season when demands are highest, and that there is a limit to how much water can be withdrawn from the root zone. There clearly is a limit to shallow (<1 m) soil-water supply during the dry season, at which time plants must rely on deep groundwater storage. If the saturation deficit in the soil becomes too great during the dry season, it takes longer for the system to 'wet up' once the wet season commences. Additional evapotranspiration also could be derived from the canopy, a process that is not well represented in this modelling but which could increase evaporative efficiency.

ACKNOWLEDGEMENTS

The authors gratefully acknowledge funding from the U.S. Geological Survey WEBB program, the Smithsonian Tropical Research Institute and U.S. AID. The Hydrology and Fluid Dynamics Group at Lancaster University generously provided the TOPMODEL Fortran source code (TMOD9502) that serves as the basis for this work. Additionally, we would like to thank Steve Paton, Raúl Rios, Ellen Axtmann, Deborah Martin and Andrés Marín for help on data collection and analysis. Shemin Ge and James Syvitski provided both facilities and guidance that aided in the completion of this work. We would also like to thank David Wolock, Richard Webb, Helmut Elsenbeer and two anonymous reviewers for their careful and extremely constructive review comments.

REFERENCES

Ambroise B, Beven K, Freer J. 1996. Towards a generalization of TOPMODEL concepts: topographic indices of hydrologic similarity. *Water Resources Research* **32**: 2135–2145.

Beven K. 1993. Prophesy, reality and uncertainty in distributed hydrological modeling. *Advances in Water Resources* **16**: 41–51.

Beven K, Binley A. 1992. The future of distributed models—model calibration and uncertainty prediction. *Hydrological Processes* **6**: 279–298.

Beven K, Kirkby M. 1979. A physically-based variable contributing area model of basin hydrology. *Hydrological Sciences Bulletin* **24**: 43–69.

Beven K, Lamb R, Quinn P, Romanowicz R, Freer J. 1995a. TOPMODEL. In *Computer Models of Watershed Hydrology*, Singh VP (ed.). Water Resources Publications: Littleton, CO; 627–668.

Beven K, Lamb R, Quinn P, Romanowicz R, Freer J. 1995b. *TOPMODEL and GRIDATB: A User's Guide to the Distribution Versions*. Technical Report TR110 (2nd edn), Centre for Research on Environmental Systems and Statistics, Lancaster University: Lancaster.
Birkeland PW. 1984. *Soils and Geomorphology*, 2nd edn. Oxford University Press: New York; 372.
Bonell M, Gilmour DA. 1978. The development of overland flow in a tropical rainforest catchment. *Hydrological Sciences Bulletin* **26**: 1–18.
Boyer EW, Hornberger GW, Bencala KE, McKnight DM. 2000. Effects of asynchronous snowmelt on flushing of dissolved organic carbon: a mixing model approach. *Hydrological Processes* **14**: 3291–3308.
Campling P, Gobin A, Beven K, Feyen J. 2002. Rainfall–runoff modelling of a humid tropical catchment: the TOPMODEL approach. *Hydrological Processes* **16**: 231–253.
Chappell NA, Franks SW, Larenus J. 1998. Multi-scale permeability estimation for a tropical catchment. *Hydrological Processes* **12**: 1507–1523.
Christophersen N, Neal C, Hooper RP, Vogt RD, Andersen S. 1990. Modeling streamwater chemistry as a mixture of soilwater end-members—a step towards 2nd-generation acidification models. *Journal of Hydrology* **116**: 307–320.
Dietrich WE, Windsor DM, Dunne T. 1982. Geology, climate and hydrology of Barro Colorado Island. In *The Ecology of a Tropical Forest: Seasonal Rhythms and Long-term Changes*, Leigh EG, Rand SA, Windsor DM (eds). Smithsonian Institution Press: Washington, DC; 21–46.
Elsenbeer H. 2001. Hydrologic flowpaths in rainforest soilscapes—a review. *Hydrological Processes* **15**: 1751–1759.
Elsenbeer H, Lack A. 1996. Hydrological pathways and water chemistry in Amazonian rain forests. In *Advances in Hillslope Processes*, Anderson MG, Brooks SM (eds). Wiley: New York; 939–959.
Elsenbeer H, Vertessey R. 2000. Stormflow generation and flowpath characteristics in an Amazonian rain forest catchment. *Hydrological Processes* **14**: 2367–2381.
Elsenbeer H, West A, Bonell M. 1994. Hydrologic pathways and stormflow hydrochemistry at South Creek, northeast Queensland. *Journal of Hydrology* **162**: 1–21.
Elsenbeer H, Lorieri D, Bonell M. 1995. Mixing model approaches to estimate storm flow sources in an overland flow-dominated tropical rain-forest catchment. *Water Resources Research* **31**: 2267–2278.
Foster RB, Brokaw NV. 1982. Structure and history of vegetation on Barro Colorado Island. In *The Ecology of a Tropical Forest: Seasonal Rhythms and Long-term Changes*, Leigh EG, Rand SA, Windsor DM (eds). Smithsonian Institution Press: Washington, DC; 95–100.
Franchini M, Wendling J, Obled C, Todini E. 1996. Physical interpretation and sensitivity analysis of the TOPMODEL. *Journal of Hydrology* **175**: 293–338.
Freer J, Beven K, Ambroise B. 1996. Bayesian estimate of uncertainty in runoff production and the value of data: an application of the GLUE approach. *Water Resources Research* **32**: 2161–2173.
Guntner A, Uhlenbrook S, Siebert J. 1999. Multi-criterial validation of TOPMODEL in a mountainous catchment. *Hydrological Processes* **13**: 1603–1620.
Hooper RE, Christophersen N, Peters NE. 1990. Modeling streamwater chemistry as a mixture of soil water end-members–an application to the Panola Mountain Catchment, Georgia, USA. *Journal of Hydrology* **116**: 321–343.
Hornberger GM, Bencala KE, McKnight DM. 1994. Hydrological controls on dissolved organic-carbon during snowmelt in the Snake River near Montezuma, Colorado. *Biochemistry* **25**: 147–165.
Igorlusecu I, Musy A. 1997. Generalization of TOPMODEL for a power law transmissivity profile. *Hydrological Processes* **11**: 1353–1355.
Johnsson MJ, Stallard RF. 1989. Physiographic Controls On Sediments Derived From Volcanic and Sedimentary Terrains on Barro Colorado Island, Panama. *Journal of Sedimentary Petrology* **59**: 768–781.
Jones JAA. 1997. Pipeflow contribution areas and runoff response. *Hydrological Processes* **11**: 35–41.
Kirkby MJ. 1997. TOPMODEL: a personal view. *Hydrological Processes* **11**: 1087–1097.
Kursar TA, Wright ST, Radulovich R. 1995. The effects of the rain season and irrigation on soil water and oxygen in a seasonal forest in Panama. *Journal of Tropical Ecology* **11**: 497–515.
Larsen MC, Torres-Sanchez AJ. 1990. Rainfall soil moisture relations in landslide-prone areas of a tropical rainforest, Puerto Rico. In *Tropical Hydrology and Caribbean Water Resources, Proceedings of the International Symposium on Tropical Hydrology Fourth Caribbean Islands Water Resources Congress*, San Juan, Puerto Rico, July 23–27.
Leavesley GH, Lichty RW, Troutman BM, Saindon LG. 1983. *Precipitation–Runoff Modeling System—User's Manual*. Water Resources Investigation Report 83–4238, U.S. Geological Survey: Denver, CO; 207.
Litaor MI. 1988. Review of soil solution samplers. *Water Resources Research* **24**: 727–733.
Molicova H, Grimaldi M, Bonell M, Hubert P. 1997. Using TOPMODEL towards identifying and modelling the hydrological patterns within a headwater tropical catchment. *Hydrological Processes* **11**: 1169–1196.
Morel FMM. 1983. *Principles of Aquatic Chemistry*. Wiley: New York; 446.
Piñol J, Beven K, Freer J. 1997. Modeling the hydrological response of Mediterranean catchments, Prades, Catalonia: the use of distributed models as aids to hypothesis formulation. *Hydrological Processes* **11**: 1287–1306.
Rice KC, Hornberger GM. 1998. Comparison of hydrochemical tracers to estimate source contributions to peak flow in a small, forested, headwater catchment. *Water Resources Research* **34**: 1755–1766.
Reynolds WD, Elrick DE. 1985. *In situ* measurement of hydraulic conductivity, sorptivity and the alpha parameter using a Guelph permeameter. *Soil Science* **140**: 292–302.
Reynolds WD, Elrick DE, Topp GC. 1983. A reexamination of the constant head well permeameter method for measuring hydraulic conductivity above the water table. *Soil Science* **136**: 250–268.
Robson A, Beven K, Neal C. 1992. Towards identifying sources of subsurface flow: a comparison of components identified by a physically based runoff model and those determined by chemical mixing techniques. *Hydrological Processes* **6**: 199–214.
Rutter AJ, Morton AJ, Robins. 1975. A predictive model of rainfall interception in forests II: Generalization of the model and comparison with observations in some coniferous and hardwood stands. *Journal of Applied Ecology* **12**: 327–380.

Saulnier GM, Beven KJ, Obled C. 1997. Including spatially variable soil depths in TOPMODEL. *Journal of Hydrology* **202**: 158–172.
Scanlon TM, Raffensperger JP, Hornberger GM. 2001. Modeling transport of dissolved silica in a forested headwater catchment: Implications for defining the hydrochemical response of observed flow pathways. *Water Resources Research* **37**: 1071–1082.
Smela SJ. 1987. *The influence of soil cracking on Radun-222 flux from a Panamanian soil*. Undergraduate thesis. Princeton University: Princeton, NJ. USA.
Soil Moisture Equipment Corporation. 1986. *2800KI Guelph Permeameter Operating Instructions*, Rev 8/8C. Soil Moisture Equipment Corporation: Goleta, CA, USA.
Stallard RF, Edmond JM. 1983. Geochemistry of the Amazon 2: the influence of the geology and weathering environment on the dissolved load. *Journal of Geophysical Research* **88**: 9671–9688.
Stallard RF, Koehnken L, Johnsson MJ. 1991. Weathering processes and the composition of inorganic material transported through the Orinoco River system, Venezuela and Colombia. *Geoderma* **51**: 133–165.
Sternberg LS, Mulkey SS, Wright SJ. 1989. Ecological interpretation of leaf carbon isotopes: influence of respired carbon dioxide. *Ecology* **70**: 1317–1324.
Uchida T, Kosugi K, Mizuyama T. 1999. Runoff characteristics of pipeflow and effects of pipeflow on rainfall-runoff phenomena in a mountainous watershed. *Journal of Hydrology* **222**: 18–36.
Windsor DM. 1990. *Climate and Moisture Availability in a Tropical Forest, Long Term Records for Barro Colorado Island Panama*. Smithsonian Contributions to the Earth Sciences 29, Smithsonian University Press: Washington, DC, 145.
Wolock DM. 1993. *Simulating the Variable Source Area Concept of Streamflow Generation with the Watershed Model TOPMODEL*. Open File Report 93–4124, U.S. Geological Survey: Lawrence, KS; 33.
Wolock DM. McCabe GJ. 1995. Comparison of single and multiple flow direction algorithms for computing topographic parameters in TOPMODEL. *Water Resources Research* **31**: 1315–1324.
Woodring WP. 1958. *Geology of Barro Colorado Island, Canal Zone*. Smithsonian Miscellaneous Collections 135, Smithsonian Institution: Washington, DC.
Wright SJ, Cornejo FH. 1990. Seasonal drought and leaf fall in a tropical Forest. *Ecology* **71**: 1165–1175.